Final Technical Report

Development of a High Resolution Imaging Spectrometer

Period of Performance : September 4, 1999 through March 4, 2000

Allen S. Krieger and Daniel R. Parsignault

Radiation Science, Inc.

P.O. Box 293

Belmont, MA 02478

Prepared for

The U.S. Department of Energy

Under Award No. DE-FG02-99ER82868

DOE Patent Clearance Granted

11/17/00

Daniel D. Park
Date

(630) 252-2308
E-mail: daniel.park@ch.doe.gov
Office of Intellectual Property Law
DOE Chicago Operations Office

DISCLAIMER

DISCLAIMER

Portions of this document may be illegible in electronic image products. Images are produced from the best available original document.

Abstract

In this program we demonstrated that a quartz crystal could be bent to a spherical shape around a convex form, thereby eliminating the problems of deviations in the flatness of the crystal, non-uniformities in crystal thickness, and variations in the thickness of the epoxy bonding the crystal to its support form. Optical testing showed that the front surface of the crystal was spherical with an RMS deviation of 1/20 of a wave. X-ray testing showed that the resolving power of this crystal was on the order of 10^4 . We developed a design concept for a spherical crystal spectrometer for use at NSTX and established that it could be built at a cost within the parameters of phase II.

Table of Contents

Abstract 1
1. Introduction 2
2. Background 3
3. The Optics of Spherically Curved Crystals 5
4. Anticipated Benefits 7
5. Phase I Technical Objectives 10
6. The Spherically Bent Crystal 12
6.1 The Crystals. 13
6.2 The Bending Technique. 13
6.3 Optical Testing. 16
6.3.1 Surface Radius Measurement. 17
6.3.2 Reflected Wavefront Accuracy (RWF). 17
6.4 X-ray Testing. 19
6.4.1 Experimental Setup. 19
6.4.2 Results: 20
7. Instrument Design 23
8. Conclusions 25

1. Introduction

Radiation Science was awarded a phase I SBIR grant to investigate the use of spherically bent crystals in X-ray plasma diagnostics. The objective of this program was to develop a new type of high resolution, crystal spectrograph for extended X-ray sources such as experimental magnetic fusion machines, e.g. tokamaks and spherical torus experiments. Specifically, we proposed to build an imaging spectrometer that could be used to measure the distribution of ion temperature and density as a function of position over the core of the National Spherical Torus Experiment (NSTX).

This project built on our previous work with large area, double focusing crystals for plasma diagnostics, DE-FG02-96ER86046. In that project, a team of scientists and engineers from Radiation Science, Inc. and the Princeton University Plasma Physics Laboratory (PPPL) demonstrated that it was possible to bend a very large crystal into an optical quality segment of a sphere, and to hold it in that shape indefinitely, (more than a year). We proposed to use such a crystal as a high sensitivity, double focusing X-ray spectrometer for extended X-ray sources.

In the present project, we used a particular property of a spherically bent, double focusing crystal spectrometer at a Bragg angle of 45° degrees. At that angle, a parallel beam of X-rays can be focused at a point, or conversely, a point source of X-rays can be collimated in a plane. The first case, makes it possible to build a high resolution imaging spectrometer for a limited range of wavelengths that includes diagnostically important lines providing simultaneous information on plasma conditions over a large plasma volume. The collimating property of the reverse configuration could have important implications for X-ray lithography from point sources such as laser generated plasmas.

The spectral lines of helium-like argon, Ar XVII, and the associated dielectronic satellites, from the lithium-like ion, are of particular interest for NSTX. These lines, which fall into the narrow wavelength range from 3.9494 Å to 3.9944 Å, provide data on crucial plasma parameters over the temperature range between 400 eV and nearly 3 keV.

The diagnostic applications include Doppler measurements of ion temperature and plasma rotation, as well as measurements of electron temperature, ion charge state distributions, and ion transport.

The main advantage of this new type of spectrometer is that it provides a spatially and spectrally resolved image of the plasma by using only one spherically bent crystal and a two dimensional detector. This crystal replaces an entire array of crystals that was used in previous instruments to obtain spatial resolution. Thus, it eliminates the need for a cross calibration of the experimental data from different radial chords. It also offers a substantial saving in cost relative to an array.

During Phase I of this program, we developed a new technique for bending a quartz crystal into the segment of a sphere of appropriate radius. Subsequent testing of the bent crystal, both optically and in X-rays, showed that the crystal was of the required quality to be incorporated in a double focusing, wavelength dispersing, high resolution spectrometer. This was a significant achievement because the quality of large size spherically bent crystals has been disappointing. In at least one case, the spherically bent crystal was less effective than the cylindrical crystal it was meant to replace. A previous design concept was then amplified as the preliminary design for the National Spherical Torus Experiment (NSTX.) imaging spectrometer

2. Background

X-ray spectroscopy has made invaluable contributions to the plasma diagnosis of magnetic confinement fusion experiments by observing the spectra of medium Z elements ($18 \leq Z \leq 36$). These elements exist in magnetic confinement plasmas either as indigenous metal impurities (Ti, Cr, Fe, and Ni) or as trace elements which are introduced in small controllable amounts for diagnostic purposes (Ar, Kr, or metals). The importance of the medium Z elements derives from the fact that they are not fully ionized in the hot core of the plasma so that the emitted line radiation can be used for measurements of the central plasma parameters. The main diagnostic applications are measurements of the central ion temperature and plasma rotation velocity from the Doppler width and Doppler shift of the observed lines. In addition, X-ray line ratios are used for determination of the central electron temperature, the ionization balance, and ion transport. The simplicity and attainable accuracy of X-ray spectroscopic methods is still unparalleled by other diagnostic techniques. Recent studies have shown that the spectra of helium-like ions can also serve as a diagnostic for the electron energy distribution. This adds to the physical parameters that can be inferred from high resolution X-ray spectra. It is especially important for studies of current-drive and profile modification experiments as well as for electron heating experiments. These features (and the fact that the instrumental equipment is relatively inexpensive) make crystal spectroscopy attractive to spheromaks as well as tokamaks.

Unfortunately, current X-ray spectrometers have a drawback. Although crystal spectrometers have produced very accurate data on the central plasma parameters, they have not yet provided the spatial resolution achieved by visible light spectrometers where supplementary imaging optics are easy to use. The problem is the geometry of the diffracting crystals.

The crystals currently used for high resolution spectroscopy are bent cylindrically in the plane of dispersion (*Johann* configuration).This configuration has been the most widely used in the spectroscopy of extended plasma sources. It provides focusing of *meridional* X-rays in the plane of dispersion, along the *Rowland circle.* But, the Johann configuration does not provide focusing for rays which are oblique to this plane, *sagittal* rays. This has two detrimental effects. First, there is a considerable loss of intensity because rays that diverge from the plane of dispersion continue to diverge after diffraction. Second, because these sagittal rays are not focussed, cylindrical crystal X-ray spectrometers capture radiation from only one line of sight through the plasma. Information on the spatial distribution of plasma parameters, e.g. the radial profile of the ion temperature, can only be obtained by using an array of spectrometers, each viewing a different chord through the plasma. Practical considerations limit the number of spectrometers, i.e. the number of lines of sight through the plasma, to a total of about five. The spatial resolution provided by such an array is not comparable to the resolution that can be obtained with visible light systems. Attempts to solve this problem by installing a slit in the plane of the Rowland circle, i.e. a one dimensional pinhole camera, have been defeated by the large difference in intensity between the central chord and the outer chords.

In our proposal, we had suggested a new type of X-ray imaging crystal spectrometer based on the optical properties of spherical crystals. In an earlier project, Radiation Science, in coordination with investigators at the Princeton Plasma Physics Laboratory, considered the development of a double focusing X-ray spectrometer, to be used in the X-ray diagnostics of existing and future fusion experiments, incorporating a spherically or toroidally bent crystal. The double focusing concentrates diverging radiation in the diffraction plane. Therefore a double focusing spectrometer would have higher X-ray throughputs to accommodate the lower impurity levels of the new machines, and would permit higher time resolution measurements. During the course of that investigation, we realized that the optical properties of Bragg reflection from a sphere at 45° provided a unique and important opportunity.

At a Bragg angle of 45° it is possible to focus a bundle of rays that are converging in the meridional plane and parallel in the sagittal plane to a point on the Rowland circle. A bundle of parallel (sagittal) rays emerging from the plasma at an angle oblique to the plane of the Rowland circle (i.e. above or below the central plane) is focussed to a point below or above the central diffraction plane proportional to the angle of the ray bundle. The extent of the cross section of the plasma that is imaged to a point on the detector is defined by the size of the crystal in the sagittal direction.

This crystal configuration has some unique advantages:

1. A large number of radial chords through the plasma can be observed with only one spectrometer having a spherically bent crystal.
2. The photons from each radial chord are reflected by the entire crystal. Local inhomogeneities of crystal properties do not perturb the spectral data from any specific radial chord.
3. The throughput of a spectrometer with a spherical crystal is significantly enhanced compared to that of a cylindrical crystal.

Moreover, used in tandem, two spherical crystal imaging spectrometers can measure the polarization of the emitted lines.

These characteristics are very important in observations of the plasma in NSTX. This machine is one of the first of a new class of magnetic confinement devices, the spherical torus. The spherical torus combines the properties of tokamaks and spheromaks. This design may have significant advantages for magnetic confinement fusion. Substantially less is known about the physics of these devices than is known about tokamaks. Thus, NSTX is an opportunity to investigate these new machines. Problems of particle and energy confinement and transport are important areas of research for this machine. Analysis of information on ion temperature and ion rotation as a function of position will be important in analyzing particle and power balance.

The main diagnostic for ion temperature in tokamaks like TFTR, the Tokamak Fusion Test Reactor, has been the use of Charge Exchange Recombination Spectroscopy (CHERS). The CHERS spectrometer monitors spectra in the visible range due to recombination of ions colliding with the neutral beams injected into the plasma. Unfortunately, when injected at the levels required for the measurement, the neutral beam particles perturb the ambient plasma. This argues against the use of the CHERS diagnostic during experiments examining alternative heating methods. High throughput X-ray spectra would satisfy this requirement. However, the requirements for high temporal and spectral resolution measurements along a number of lines of sight through the torus indicate that a new spectrometer design is needed.

3. The Optics of Spherically Curved Crystals

In this section, we compare the properties of cylindrically curved crystals with those of spherically and toroidally curved crystals. Figure 1 (from an early paper by Hill *et al*) shows the standard Johann spectrometer with a cylindrically curved crystal, as it has been used in most tokamak experiments. The radius of curvature of the crystal is twice that of the Rowland circle, so that the crystal touches the Rowland circle only at one point. Radiation in the plane of the Rowland circle of a given wavelength passes through a beryllium window to the crystal and is Bragg reflected and focused to a point on the detector. The lengths of the window and of the counter determine the wavelength range which can be obtained for one setting of the central Bragg angle. The height of the window, w, above and below the Rowland circle, determines the intensity.

In this configuration, there is no focusing perpendicular to the Rowland circle. The radiation from the plasma continues to diverge in this direction between the crystal and the detector. This results in a loss of intensity which can only be recovered by increasing the vertical size of the detector. If the aperture of the spectrometer is open, it is impossible to determine the vertical position of the source of the X-rays from the position at which they strike the detector.

A substantial enhancement of the intensity may be expected from the use of spherically bent crystals relative to the Johann configuration. Spherically bent crystals provide focusing in the vertical direction and maintain the essential focusing properties of the

Johann configuration for the horizontal rays. It was this enhancement in the intensity that motivated our previous work on spherically bent crystals.

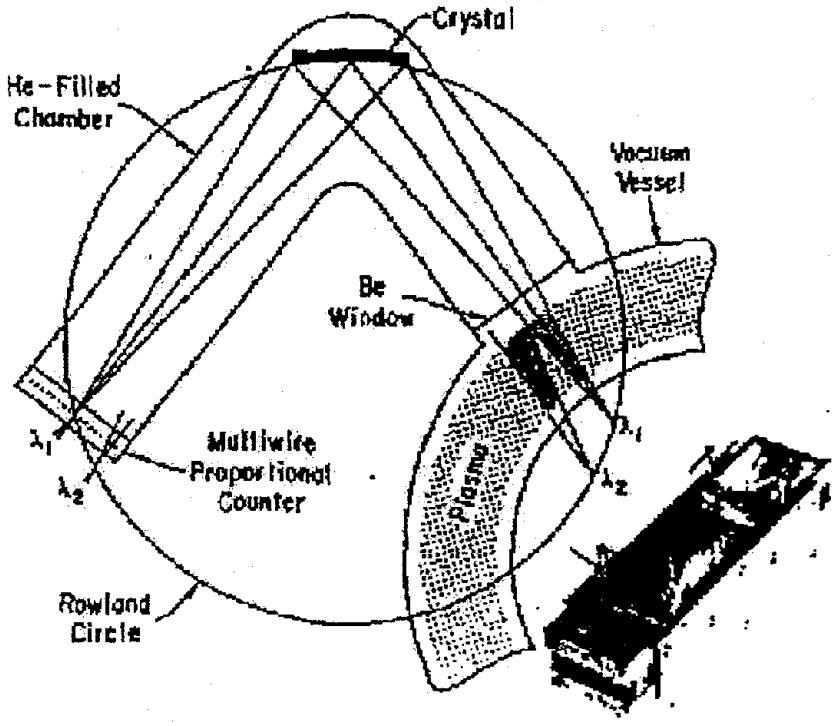

Figure 1: A cylindrically bent crystal spectrometer

The focusing properties of spherically bent crystals for rays in the meridional (horizontal) plane and the central sagittal (vertical) plane are illustrated in Figure 2. The center of the crystal touches the Rowland circle at **C** . The crystal curvature radius, R, is twice the radius of the Rowland circle so that the center of the crystal sphere is at **O**, which is also on the Rowland circle. F_m is the focal point in the meridional plane and F_s is the focal point in the central sagittal plane which intersects the crystal along the line **CB**. Rays in these planes, which pass through F_m and F_s, are reflected from the crystal and focused to a point on the Rowland circle at **A**, the center of the detector. The ratio of the sagittal and meridional focal lengths, f_s/f_m is a function of the Bragg angle, θ, given by

$f_s/f_m = \dfrac{-1}{\cos 2\theta}$ with, $f_M = R_C \sin\theta$ where R_C is the radius of curvature of the crystal.

These relations can be derived by examination of Figure 2. The triangles **OCA** and **OBA** are identical triangles, which can be superimposed by a rotation about the axis **OA**. A ray incident on **B** and detected at **A** must be in the plane of triangle **OBA**, which contains the normal **OB** to the crystal at point **B**. From the Bragg condition, the angle Ψ between the incident and reflected rays at **B** is $\Psi = 180° - 2\theta$. The sagittal focal point, F_s, from which the incident ray emerges, must be on the line **OA**, which is common to the meridional plane **OCA** and the tilted plane **OBA**.

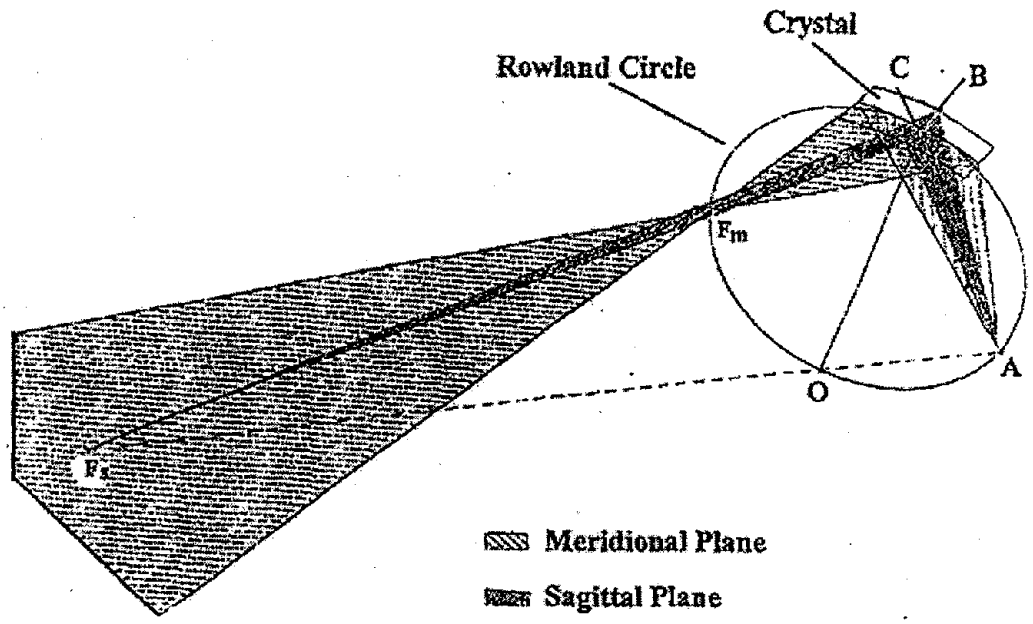

Figure 2: The focussing properties of spherically bent crystals

This equation has important consequences for the design of a crystal spectrometer. The ratio f_s/f_m is negative for $\theta < 45°$ (divergent sagittal rays) and positive for $\theta > 45°$ (convergent sagittal rays); for $\theta = 45°$, the sagittal rays are parallel. A bundle of sagittal rays, parallel to the plane of dispersion, will be focussed to the point F_m on the Rowland circle. A bundle of parallel (sagittal) rays that is oblique to the diffraction plane is focused to a point above or below the central diffraction plane. Thus, a measurement of the intensity of a spectral line, as a function of position perpendicular to the plane of dispersion at the detector, is a measurement of the emission at that wavelength along a line of sight at an angle to the dispersion plane given by the height of the point on the detector. This is precisely the performance of a visible light optic for a parallel beam. Line width measurements as a function of height on the detector are measurements of T_i as a function of position within the plasma. Measurements of wavelength shift as a function of height are measurements of ion velocity along the line of sight as a function of position. If there are a group of lines diffracted at Bragg angles close to 45°, and the physics of their formation is well understood, line ratios provide n_i, T_e and n_e. If a two-dimensional detector is used, all these measurements are made simultaneously.

4. Anticipated Benefits

The objective of the combined phase I and phase II program was the construction of a spherically bent crystal spectrometer for measurements of the spectrum of helium-like argon, at NSTX.

NSTX is one of the first examples of a new class of magnetic confinement fusion device, the Spherical Torus. As such, it is of great interest, both in terms of the physics of the plasma regime that it will explore, and also, the engineering of machines of this type.

These machines will combine the features of conventional tokamaks with those of the Spheromak, a compact toroidal device. Spherical torus devices are expected to ultimately achieve higher densities and temperatures than tokamaks of the same size. NSTX is designed to provide fundamental information on the properties of these devices. If it is successful, the spherical torus design principle will lead to small fusion power sources to help address a wide range of energy-related challenges.

This spectrometer will be designed to make high resolution measurements of X-ray line profiles along varying lines of sight through the torus from a trace element injected into the plasma. From the line profiles, spectroscopists can determine the core ion temperature as well as the spatial distribution of ion temperatures within the non-circular NSTX cross-section. The displacements of the line centroids from their stationary locations along various lines of sight will provide a measure of plasma rotation velocities. Line ratios will provide the ion charge state distribution, and hence, the electron temperature. These measurements will contribute to the understanding of energy and particle confinement and fluxes in NSTX. Because this diagnostic does not depend on the presence of a neutral beam as CHERS does. It can be used under circumstances where the neutral beam would perturb the plasma and disguise the effects under study, e.g. the study of alternative heating mechanisms.

Argon is a good choice for the injected impurity. NSTX is designed to have a central temperature of 1 to 2 keV. Figure 3 shows the abundance of the ionization states of argon as a function of temperature under the assumption of "coronal equilibrium". Helium-like Ar^{16+} exists over a wide range of temperatures. It is the most prevalent argon ion in the plasma temperature range from 0.3 keV to 3 keV. In addition, because it is a gas, argon injection can be controlled more precisely than evaporated metals.

The spectra of helium-like ions offer a special opportunity to determine the characteristics of the emitting plasma. Figure 4 shows a spectrum of the region covering the resonance, recombination, and forbidden lines of helium-like argon along with the neighboring satellite lines due to dielectronic recombination from the lithium-like ion. This spectrum was obtained at TEXTOR in Julich, Germany with a Johann spectrometer based on the TFTR design and using equipment from the TFTR spectrometers. The plasma parameters of NSTX are expected to be similar to those of TEXTOR. The lines are labeled with the Gabriel notation.

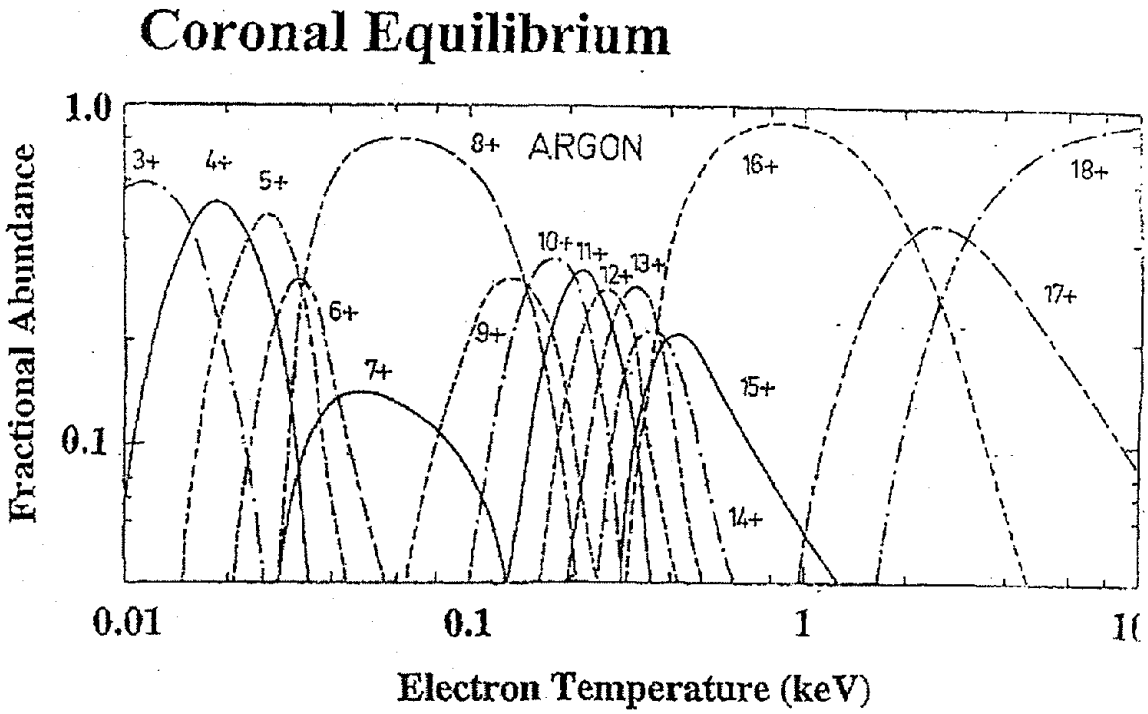

Figure 3: The fractional abundance of Ar ions as a function of electron temperature

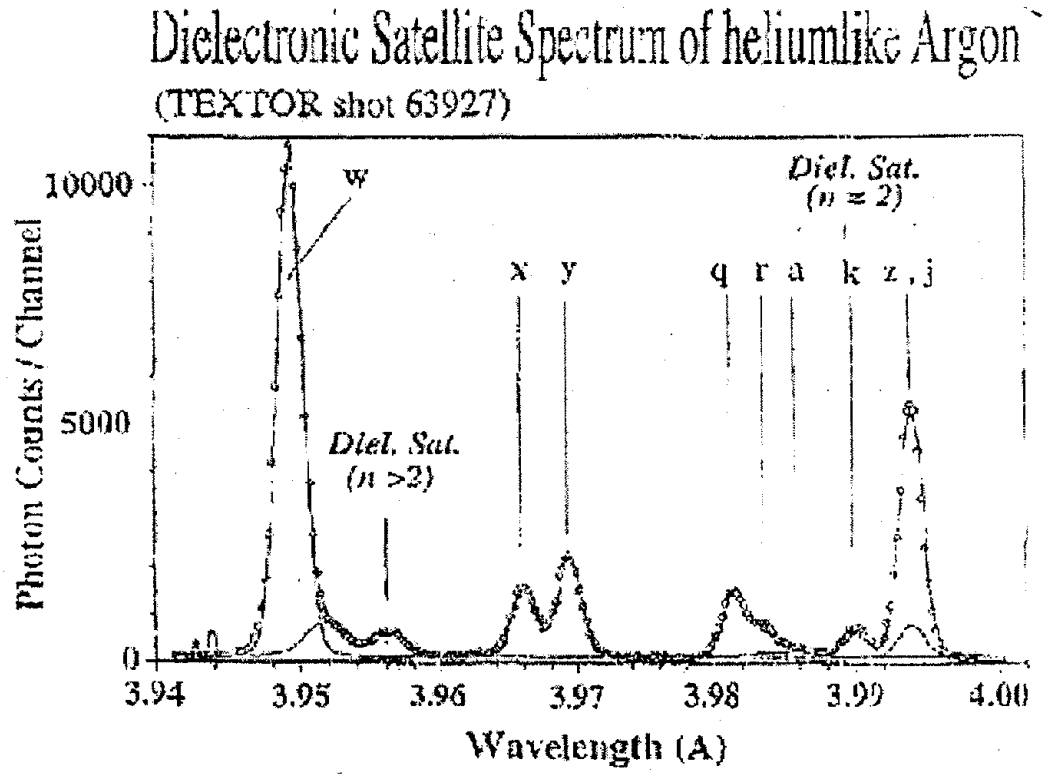

Figure 4: High resolution spectrum of the resonance line spectrum of He-like Ar.

The line labeled W is the $1s2s(^1S_0)$-$1s2p(^1P_1)$ resonance line of 16 times ionized helium-like argon (Ar XVII) along with the associated intercombination and forbidden lines (X, Y and Z) and the associated lithium-like satellite lines produced by dielectronic recombination. The solid line represents a list squares fit to the wavelengths of Vainshtein and Safronova Ion temperatures, electron temperatures and plasma toroidal velocity during sawtooth oscillations have been obtained at TEXTOR with a resolution of 1 msec from helium-like argon spectra.

The NSTX instrument will be much more sensitive than the TEXTOR design, with no increase in size, because it will use a spherically bent crystal and a two dimensional imaging detector. It will be possible to obtain more accurate determinations of the ion temperature, the electron energy distribution, and the toroidal rotation velocity along a plethora of chords perpendicular to the line of sight. These measurements will be made with higher time resolution using less than 10^{-3} Torr-L/sec of injected argon. Perturbation of the plasma will be minimal.

A fast soft X-ray camera, using a 10 cm diameter image tube and a special CCD, has been used to image the Ar spectrum with 16 msec exposures. Figure 5 shows the images obtained from eight individual shots at TEXTOR. The images from shots 4 and 5 were distorted by interference. The images from the other six shots, however, show that the lines are easily resolved and detected with ample signal-to-noise by this detector. The data from the line images perpendicular to the Rowland circle do not represent images of the plasma because a cylindrical crystal was used. This detector had ample sensitivity for these spectra.

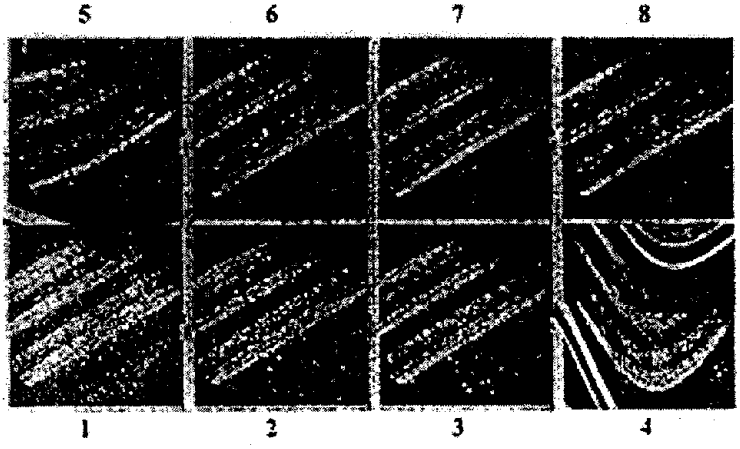

Figure 5: Two dimensional images of single shot argon spectra from TEXTOR

5. Phase I Technical Objectives

Radiation Science together with the Princeton University Plasma Physics Laboratory, proposed to develop a spherically bent crystal imaging spectrometer for extended X-ray sources. The objective of the overall program was to design and build a prototype imaging spectrometer, tuned to the resonance line of helium-like argon and its satellites, which could be used to measure the ion temperature, plasma rotation, and ion density at

NSTX. This prototype would demonstrate the value of this technique for use at future large scale fusion reactors such as ITER. The specific objectives of the Phase I program were:

1. To develop a precision bending technique that does not require a pressure differential to maintain the shape of the crystal.
2. Using this technique, to bend a quartz crystal with the appropriate radius of curvature and measure its optical and X-ray performances, and
3. To amplify our spectrometer design concept into a preliminary design for the NSTX imaging spectrometer.

In our previous study, we had pressed a thin silicon crystal into a concave spherical template. This template consisted of an off -the-shelf, $\lambda/4$ spherical mirror with a 6.35 meter radius of curvature. The crystal, 20 cm in diameter, was held in contact with the template by establishing a pressure differential between the crystal and the substrate. After the pumping assembly was detached, the vacuum held the back of the crystal in contact with the substrate. In the actual spectrometer, we could have substituted a helium atmosphere for the air used in our design study, in order to minimize the absorption of the X-rays.

X-ray spectra obtained at Princeton Plasma Physics Laboratory showed that the spot sizes at the meridional and sagittal foci approached the theoretical values, an indication that the crystal showed a small departure from sphericity. Optical tests at Radiation Science indicated that we had achieved only a 3/4 λ mirror. This discrepancy was caused by variations in both the flatness and in the thickness of the crystal.

Therefore, we had to find a somewhat different bending technique, which although based on our successful first attempt at bending a crystal, would yield a more precisely bent crystal. It was also obvious that the flatness and the thickness uniformity of the crystal would have to be better controlled.

The requirements of the present instrument are somewhat different than those of our previous design. At the start of the earlier work, we assumed that our crystal spectrometer would be used at ITER to examine the X-ray spectrum of helium-like krypton atoms whose average energy is 13 keV. Under these circumstances, the interior of the spectrometer would have been filled with air at about one atmosphere of pressure, which would have provided the pressure differential needed to hold the crystal in its spherical mount. However, at NSTX, the X-ray emission to be monitored is that of helium-like argon atoms whose average energy is 3 keV. The absorption coefficient of 3 keV X-rays, which is almost 2 orders-of-magnitude larger than that of 13 keV X-rays, excluded an atmosphere of air. Using an atmosphere of helium in the spectrometer chamber would have been a solution, but it was rejected for technical reasons. We were thus driven to find a crystal mounting technique, which did not require the presence of a gas-filled chamber.

Both the groups at the Kurchatov Institute, Moscow and at Jena, Germany have used smaller spherical crystals, which were bonded to their supporting forms. Our colleagues at Princeton University have tested a 4 cm x 7 cm, spherically bent, quartz crystal provided by the Russian group. Prior to the bending, the flat crystal was said to be of

high quality. However, the spherically bent, mounted crystal did not meet the accuracy requirements for this application.

The need to detect a specific element, helium-like Ar, which emits X-rays with energies around 3 keV, dictated the use of a quartz crystal instead of a silicon crystal. We had to verify theoretically and experimentally that the results obtained with a silicon wafer would be relevant to a quartz crystal. We compared analytically the mechanical behavior of a quartz crystal to that of a silicon crystal under identical conditions. The analysis showed that our technique would work equally well with a quartz crystal, despite the difference in the mechanical properties between the two materials. We had also to take into consideration that the diagnostic instruments would be closer to the plasma at NSTX than at ITER. It meant that the radius of curvature of the crystal would be about half as large in this case than in our original design, thus increasing the stress in the crystal.

Our design concept for the imaging spectrometer is also quite simple. It is based on the Argon line crystal spectrometer at TEXTOR, which uses a cylindrically bent crystal. In this case, a spherical quartz crystal is mounted in a chamber connected to the vacuum vessel of NSTX by a tube, such that it is approximately 3 meters from the plasma center. The crystal is aligned such that the Bragg angle is appropriate for reflection of the Ar XVII resonance line (actually, $\Theta = 53.95$ degrees) Another tube of length approximately equal to f_M connects the crystal chamber to that of the detector. The positions and orientations of both the crystal and the detector are adjustable for proper alignment. The final details of the design will depend on the mechanical interface with NSTX, and the electronic interface with the instrument control and data acquisition system.

6. The Spherically Bent Crystal

This task involved the design and construction of a crystal assembly which corresponded to a segment of a sphere more closely than in our previous trial, and a measurement of the X-ray imaging properties of this crystal assembly. Radiation Science designed and constructed the crystal assembly. The sphericity of the assembly was verified, using a visible light interferometric technique, and it was subsequently delivered to Princeton University Plasma Physics Laboratory for X-ray testing.

In our previous work, we had bent a 0.625 mm thick, 20 cm diameter silicon crystal into a segment of a sphere by forcing the back of the crystal into contact with a concave spherical form, a $\lambda/4$ spherical mirror with a radius of curvature of 6.350 m. We established a pressure differential of 1 atmosphere, by evacuating the volume between the crystal and the sphere. In order to do this, we drilled a 4.76 mm hole in the center of the concave form. Laser Unequal Path Interferometry (LUPI) measurements, after the crystal was mounted, showed that, while the average surface of the crystal was a faithful replica of the sphere out to a diameter of 18 cm, the remaining surface up to the edge of the crystal departed somewhat from a spherical shape, up to $3/4\lambda$. There were two causes for the loss in figure: the silicon wafer, due to internal stresses, was not flat to start with and its thickness was not uniform.

In the present work, we therefore had to insure that the quartz crystal would be as stress free as possible, and of uniform thickness. It should be remembered that the 20 cm silicon crystal was manufactured for the electronics industry, where flatness and small

non-uniformity in thickness are of no consequences, whereas in spectroscopy, these defects cannot be overlooked.

A crystal which appears satisfactory in visible light, may not perform properly in X-rays. The chemical polishing process used to flatten the crystal surfaces may introduce subsurface damage that detracts from its X-ray performance. In addition, the surface of the crystal may not be parallel to the diffracting plane. Angular differences between the surface and the crystal planes on the order of minutes of arc are common on high quality crystals.

6.1 The Crystals.

We selected three different vendors specializing in crystal manufacturing to whom we sent a request for a quotation. We eventually settled on Inrad, Northvale, New Jersey. We ordered 2 quartz crystals. Each crystals was 100 mm in diameter x 0.75 mm in thickness. The crystals were cut along the (1,1,-2,0) lattice plane, with a corresponding $2d$ spacing of 4.913 Å, resulting in a mean Bragg angle of $\Theta = 53.95^{\circ}$ for the argon lines. The parallelism between the front surface of the crystal and the lattice plane was within one arc minute. The 2 surfaces of the crystal were cut parallel to within 10 arc-second. The technique for cutting and polishing of the crystals is proprietary to Inrad.

The radius of the cylindrical crystal used at TEXTOR to spread the narrow wavelength range between 3.94 and 4.00 Å, over a 5 cm length of the Rowland circle, is 3.780 m. Figure 4 shows that the resulting argon line spectrum is easily resolved by the detector. We settled on a radius of curvature of 3.750023 m,. for practical reasons (see below)

6.2 The Bending Technique.

The standard method for generating small spherical crystals seems to involve pressing the rear surface of a planar crystal into contact with a concave form. If the crystal material is sufficiently elastic and the radius of curvature of the sphere is small enough, i.e. a deep bowl, the crystal will maintain itself in the form. If not, the crystal is cemented to the spherical form. The Moscow group uses small spherical crystals of mica to measure the spectra of laser generated plasmas. The Jena group seems to bend small quartz crystals into spherical forms with much lower $1/f$ numbers than we use.

In both of these techniques, the crystal is constrained during the mounting process at both the front and rear surfaces. There is no possibility of relieving the internal stresses which can distort the crystal planes thereby reducing the resolution. In addition, success with any method using a concave sphere behind the crystal to generate its shape requires control of the uniformity of three parameters: the thickness of the bonding agent, the thickness of the crystal, and the flatness of the crystal. If any of these characteristics is non-uniform, the front surface of the crystal will not be spherical.

In the present work, we devised a technique, which has the advantage of eliminating the influence on the final figure of non-uniformities in the flatness or thickness of the crystal, or the thickness of the bonding agent layer. In order to achieve this, we constrain the ***front*** of the crystal into a spherical configuration by forcing it against a convex spherical form. We then attach a concave support mounting to the back of the crystal. The support

behind the crystal does not define the configuration of the front surface, but simply prevents the crystal from relaxing.

To implement this technique, we procured from Janos Technology Inc., Townshend, VT, an optical test plate assembly consisting of matched plano-convex and plano-concave elements with the required radius of curvature. Fortuitously, there happens to be an optical standard with a radius of 3.750023 m, which is close enough to the approximate requirement of 3.780 m. We used these test plates as our bending forms. These Pyrex test plates had a diameter of 127 mm x 25.4 mm thick, each, with a 1/4λ or better fit to the reference sphere at 0.63 micron. These test plates had a "standard" optical surface finish.

An O-ring groove, 84.330 mm in inner diameter, 4.090 mm wide, and 3.280 mm deep was cut, in the convex piece, concentric to the axis of symmetry of the plate. Three pumping holes, 1.20 mm in diameter and equally spaced on a diameter of 76.20 mm, were drilled through, the plate to provide the vacuum connection for the vacuum pump. In addition, a circle was scribed into the surface of the convex sphere at 100 mm diameter for alignment purposes. Figure 6 is a sketch of the design of the convex spherical template.

A hole of 2.0 mm diameter was drilled through the center of the concave element so that epoxy could be injected behind the bent crystal.

The concept was that when a vacuum was applied between the convex sphere and the crystal, the "front" of the crystal would compress the O-ring until it conformed to the surface of the sphere. Then, while the front of the crystal was held in contact with the spherical surface, the concave element would be positioned behind the crystal and bonded to the back surface of the crystal. The crystal would be held in contact with the convex sphere by the vacuum until the epoxy set.

There were a number of potential problems that had to be resolved. For example:

1. Our technique relies on the ability of the crystal to compress the O-ring so that perfect contact with the convex form is achieved. This can only be accomplished over a small parameter range in the combination of O-ring compressibility and O-ring groove shape.
2. Even if we achieved perfect contact at the radius of the O-ring, the figure in its vicinity would suffer because the crystal is no longer in contact with the sphere outside the O-ring radius. This edge effect changes the effective pressure on the crystal in the vicinity of the O-ring so that perfect contact can be achieved only over a somewhat smaller radius.
3. We had to develop a technique which would hold the crystal to its support without establishing non-uniform stresses on the crystal planes which would widen the rocking curve of the crystal beyond the value expected for a uniformly bent spherical crystal.

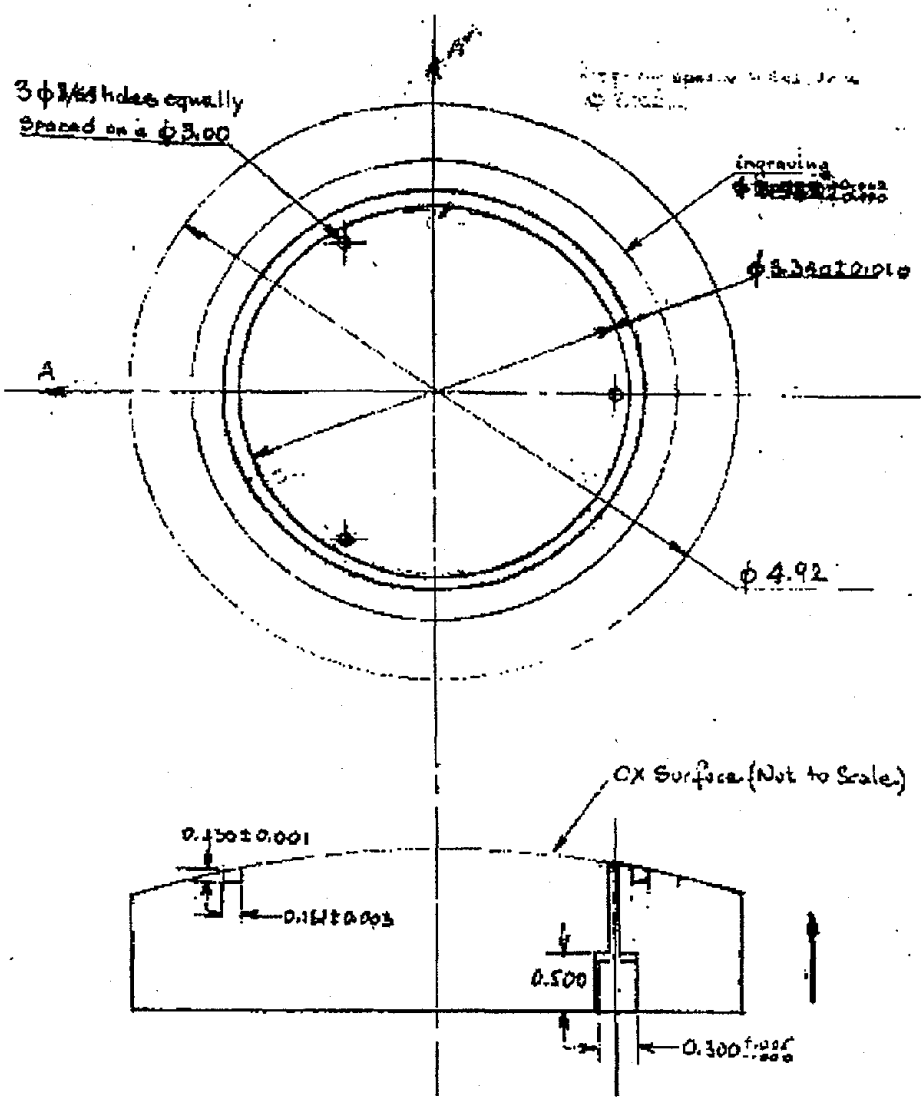

Figure 6: The convex spherical template

We first practiced our technique, using silicon wafers of 100.00 mm diameter and 0.76 mm thickness. A simple calculation had shown that, for our purposes, the mechanical properties of a silicon wafer of 0.76 mm were equivalent to that of a quartz crystal of 0.75 mm. However, these silicon wafers were standard wafers used in the electronic industry, and therefore had a "flat" cut in their circumference to indicate the orientation of the atomic planes. This flat reduced the useful diameter of the wafer to 84.74 mm. It meant that the o.d. of the O-ring groove would be 1.12 mm away from this flat edge. This, in turn, resulted in a small loss in the useful area of the quartz crystal, which otherwise could have been increased to a diameter of 90.00 mm.

During our first few trials at bending a silicon wafer on the above convex plate, interference fringes indicated that the crystal was not in perfect contact with the curved surface of the plate, beyond a diameter of about 65 mm. The O- ring was made of silicone rubber, which had a hardness of 40 (Shore 'A' durometer scale) The material of the O-

ring and the depth of the O-ring groove were chosen such that one atmosphere of pressure would bring the crystal in close contact with the convex test plate. However, because of the edge effect mentioned above, the calculations to determined the required depth of the O- ring groove were only approximate, and some adjustments had to be made. Subsequent measurements showed that an additional 0.102 mm should be added to the depth of the groove.

This modification to the O-ring groove somewhat improved the area where the crystal was in intimate contact with the test plate, to a diameter of 76.2 mm. However, fringes still appeared beyond this point, indicating that now the pumping holes were being "choked" by the crystal, and that the O-ring may still not have been completely compressed. To avoid this choking, we then machined 3 shallow grooves, each starting at one of the pumping holes and terminating at the O-ring groove. Toward the end of the program, we developed a technique for controlling the compressibility of the O-ring by cutting off a portion of the rubber O-ring, starting horizontally from the outside of its diameter toward its center, to give it a "C' shaped cross section. The contour of the C was adjusted to achieve an appropriate value for the compressibility.

These modifications were fairly successful in extending the area of close contact of the crystal with the spherical template. However, it is a physical fact that unbalanced stresses in the crystal at the position near the O- ring will always produce a departure from perfect contact in this vicinity, resulting in the useful crystal area being somewhat diminished. However, this small perturbation can be taken into account in the future design of bent crystals, by making the crystal slightly larger than the required size.

Once the crystal was bent against the convex test plate, we had to bond it to the concave plate which served as a supporting structure. We used a technique based on that used in X-ray astronomy for securing thin-walled X-ray telescope mirrors, made of low expansion materials, to their supports. The concave form was held above the crystal by shims which allowed a small gap between the back of the crystal and the glass. An epoxy, chosen for its low outgassing and coefficient of thermal expansion properties, was injected into the gap so that it would spread over the back of the crystal by capillary action. The thickness of the gap between the back of the crystal and the concave sphere had to be adjusted to the viscosity of the epoxy in order to insure uniform coverage. Laboratory tests with flats established the appropriate parameters. A precisely controlled gap of 0.178 mm was established between the two plates. A special epoxy mixture was injected into the gap. A combination of the pressure applied to inject the epoxy together with the capillary forces of the fluid between the two plates was used to fill the gap to the outside circumference of the crystal. We found that the pressure on the epoxy had to be removed immediately after injection to avoid the formation of a "high spot" in the center of the crystal due to buildup of epoxy.

6.3 Optical Testing.

The optical testing was conducted at the facilities of Telic Optics, Inc. in N. Billerica, MA. The test procedure differed from that of our previous work in that the interferometer that we used was different from the one at our previous optical testing vendor.

6.3.1 Surface Radius Measurement.

Due to the large nominal value of the radius of curvature (approx. 148 in.,) it was not possible to use the standard radius bench set-up to measure the actual value of the radius of the bent crystal, nor was it practical to use an interferometer because of the many folding mirrors required to fold the light path such that the entire test arrangement could be made on a vibration isolated laboratory test table. Therefore, a Foucault Knife Edge Tester was used, which was less sensitive to vibrations and air turbulence, and which had the advantage of not having to use folding mirrors. The radius of the bent crystal was measured to be 148.25 ± 0.125 inches (3765.6 ± 3.18 mm) compared to the template radius of 3750.023 mm. Given the large size of the radius, this is an acceptable degree of accuracy.

6.3.2 Reflected Wavefront Accuracy (RWF).

The RWF-testing was performed with an interferometer located on a vibration isolated table. The interferometer used was a Zygo GPI-XP, Mark IV, Fizeau-type interferometer. The interferometer is computer driven and produces print-outs of the data analysis from which the peak-to-valley value of the reflected wavefront accuracy can be read directly. Entering the factor of 0.5 for the ratio between the surface quality and the wavefront quality, expressed in fractions of wavelength at 0.63 microns, gives the surface accuracy, which appears on the print-out data sheet. In our initial measurement we found a 4 mm diameter high spot in the center of the crystal. This was a result of a build up of epoxy at the injection hole (see above). As expected, the performance of the mirror fell off considerably at a radius of 3.8 cm. Figure 7 shows the result when the central 4 mm of the crystal and the region beyond 7.5 cm diameter were masked off.

Project No: 4969

TELIC OPTICS, INC.
152 RANGEWAY ROAD
N. BILLERICA, MA 01862-2010

MASKED APERTURE

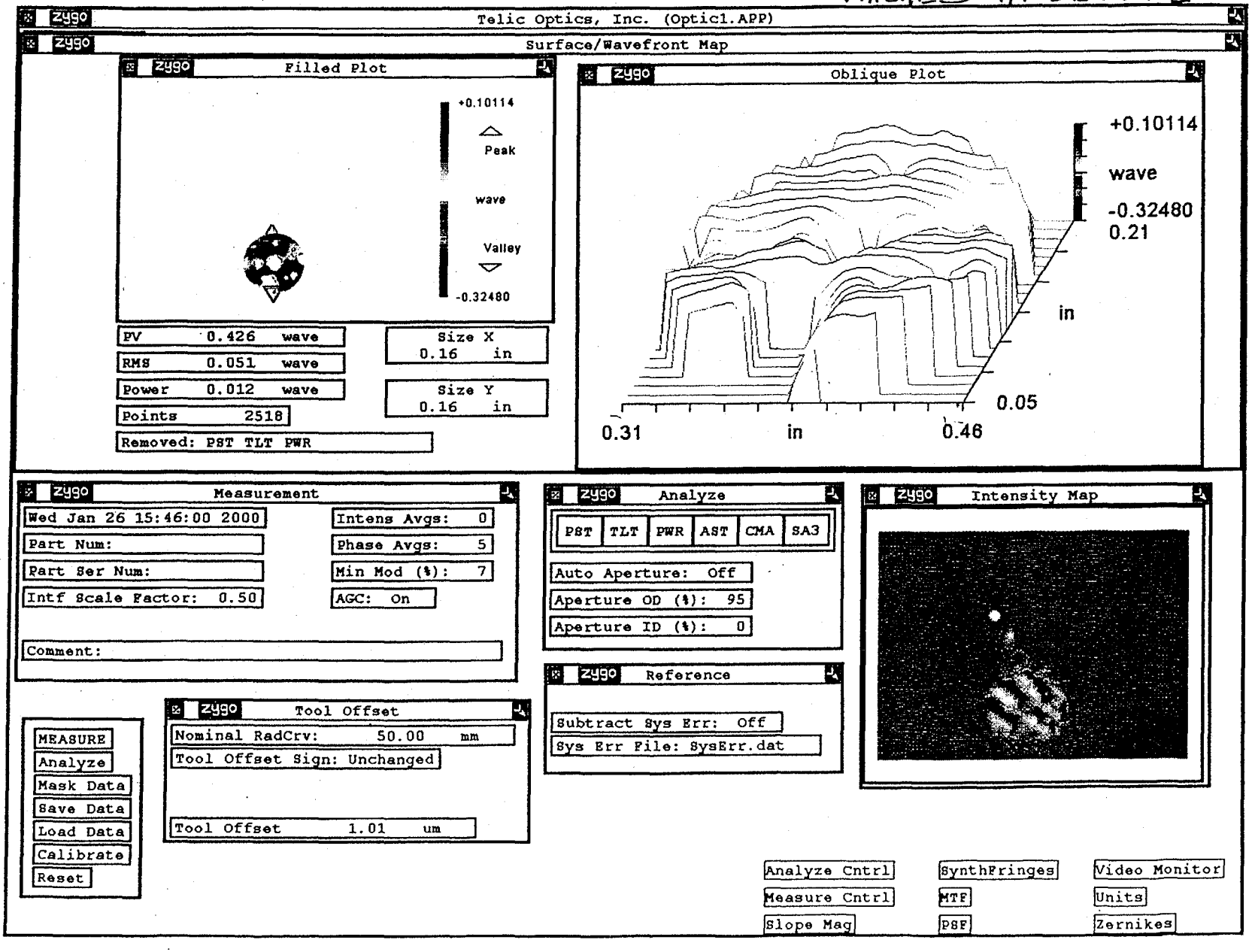

In this figure, the relevant results are:

- PV: The height between the lowest and highest point on the test surface,
- RMS: The root-mean-square deviation of all points from the best sphere fit to the test part surface, and
- Power: A measure of the low frequency deviation of the surface from the best fit sphere. Power is positive for a concave surface, and negative for a convex surface, and
- Points: The number of data points or pixels in the data set.

Note: please disregard the numbers in "size X" and "size Y" boxes, and the dimensions on the three-dimensional plots.

When the crystal was masked to an effective diameter of 7.50 cm, the Intensity Map, in the lower right corner of the figure, shows a set of parallel, and straight lines. Several little "islands" of fringes on the map indicate that unfortunately, although the crystal was assembled on a clean bench, there were still some residual dust particles, which were trapped between the crystal and the convex template. In Figure 7, the PV = 0.444 wave, and the RMS = 0.050 wave. These results show that, optically, we achieved our goal of bending the crystal, over a diameter of 7.50 cm, with the proper radius and precision in the surface figure.

6.4 X-ray Testing.

6.4.1 Experimental Setup.

The spherically bent crystal was then tested with X-rays at Princeton Plasma Physics Laboratory. The experimental setup consisted of an X-ray source, a vacuum housing, and a two-dimensional position-sensitive multiwire proportional counter to detect the diffracted X- rays.

The X-ray source was a Siemens X-ray tube with a tungsten target. It produced a spot source of X-rays 0.75 x 1.0 mm^2 in size. The emitted X-ray spectrum consists of a bremsstrahlung continuum together with the tungsten L peaks at 8.396 and 9.670 keV.

The detector was a two-dimensional imaging multiwire proportional counter (MWPC) with dimensions of 10 cm x 10 cm x 0.6 cm. The spatial resolution in the horizontal direction, i.e. in the plane of dispersion of the X-rays, was about 0.2 mm FWHM. The resolution was slightly worse in the vertical plane, ~0.3 mm FWHM. The horizontal and vertical positions of the X-rays impinging onto the detector were separately measured with a multidimensional multichannel analyzer and encoded into a 512 x 512 pixel image. The factor for conversion between photon position and channel number is about 0.24 mm/channel.

The housing consisted of two pipes welded into a cylindrical vacuum chamber containing the bent crystal. The entire assembly was evacuated to a pressure of 10^{-4} torr to minimize the absorption of X-ray between the source and the detector. The ends of the pipes were

covered with thin mylar foils of thickness ~0.001 inch to allow the X-ray to enter and exit the apparatus.

The apparatus was constructed for a Bragg angle of about 54 degrees. The radius of curvature of the quartz crystal is R = 375 cm. The distance between the crystal pole and the focus of the horizontal rays was 303 cm. The focal length of the sagittal rays was 982 cm, (effectively infinity). The X-ray source was located on the Rowland circle, and the detector was placed close to the horizontal focal point to obtain the minimum width of the diffracted X-ray line. The detector was also moved different distances away from the crystal to study the sagittal focusing behavior of the crystal by observing the decreasing height of the image with distance from the crystal.

The uniformity of the radiation field from the X-ray tube at the location of the crystal had been previously measured using a metal grid and a metal bar as masks. The radiation field was found to be uniform to ± 10% across a lateral distance of 18 cm.

During the measurements the approximate energy of the X-rays diffracted from the crystal was determined by the pulse height of the signals from the anode wires. The pulse height was calibrated with Mn K_α X-rays from an ^{55}Fe source. The pulses corresponding to diffracted X-rays were mostly in the range of 6-7 keV and 3 keV. The higher energy line agrees with the expected second order diffraction of the continuum radiation from the quartz 110 crystal, 2d=4.913Å, at an approximate Bragg angle of 54 degrees. The first order radiation near 3 keV is expected to be completely blocked by the 1-mm thick beryllium window on the X-ray tube. The observed counts near 3 keV are probably due to the argon escape peak from the argon gas in the P10 (argon-methane) mixture used in the MWPC.

6.4.2 Results:

Both the X-ray tube and the detector were placed approximately on the Rowland circle; the optimum locations were determined by positioning either the tube or the detector at different distances from the crystal until the minimum image width was obtained. The image of the X-ray source was a vertical line approximately 3.5 cm high.

The monochromatic X-ray image of the tube anode spot is illustrated in the contour plot of Fig. 8. The image is actually a very narrow vertical line, but the width of the line has been magnified by a factor of about 15 to illustrate the structure of the line. Each major division in the ordinate scale corresponds to 12 mm. The contours increase from outside to inside in increments of 1500 counts/horizontal channel, starting at 1500 counts/channel. Thus the maximum contours plotted correspond to about 10,500 counts/channel. The "streaks" in the image may be instrumental artifacts.

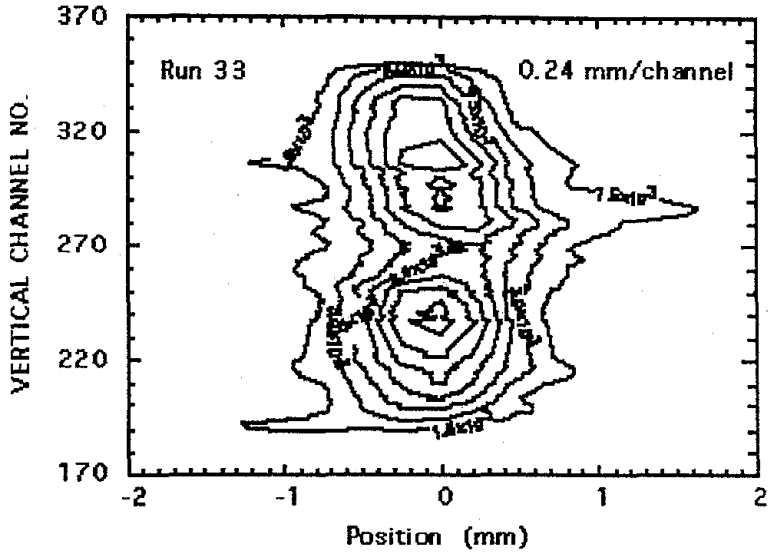

Figure 8 -- Dispersed X-ray Image. Horizontal (spectral) scale is magnified by 15X

The relevant measure of the resolving power of the crystal is the linewidth. To illustrate typical linewidths, Fig. 9 displays horizontal cross-sections of the spectral line image at different vertical positions indicated by the vertical channel numbers shown in Fig. 8. That is, the X-ray counts per horizontal channel of the image of Fig. 8 is shown as a function of horizontal position in mm for specific, selected vertical channels. The selection criterion for the vertical channel numbers was to illustrate lines of different widths ranging from the broadest to the narrowest.

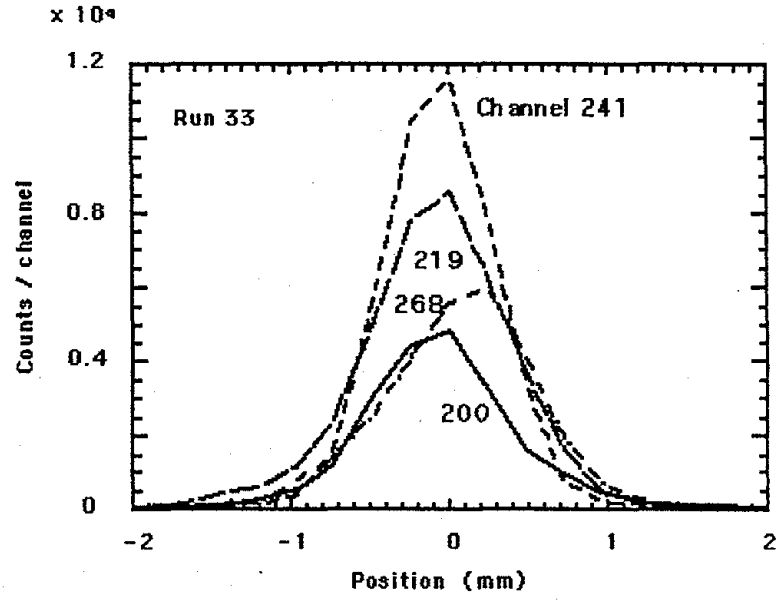

Figure 9 -- Line Profiles at Various Heights

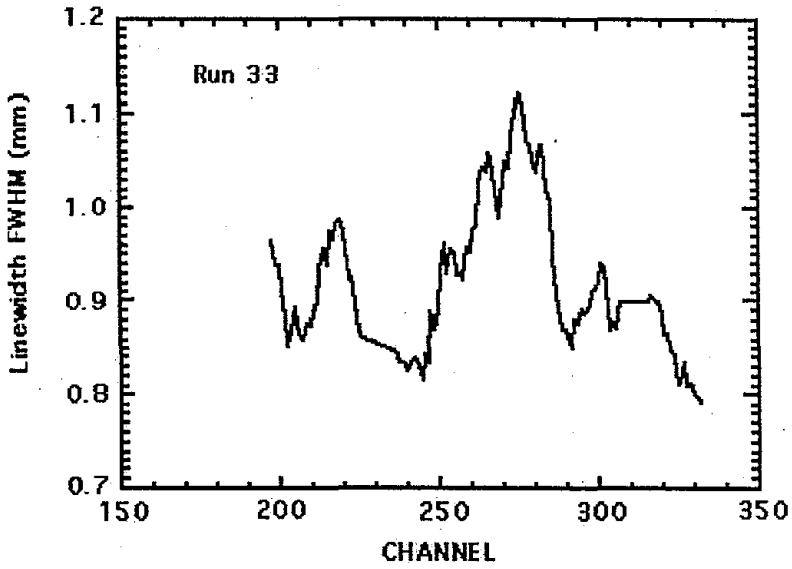

Figure 10 -- Linewidth vs. Vertical Channel Number

The width of all the horizontal lines as a function of vertical channel number are shown in Fig. 10. As noted above, the peaks in this function may be the result of instrumental artifacts. Since the anode spot of the X-ray tube has a width of about 0.75 mm, the observed linewidth is the convolution of the crystal FWHM with the anode spot size. After deconvolution one can determine the resolving power of the crystal from the relation

$$E/\Delta E = \tan\theta / \Delta\theta,$$

Where θ is about 54 degrees, and $\Delta\theta$ is determined from the crystal FWHM divided by the detector-to-crystal distance $l = R \sin\theta$. The resolving power of the crystal as a function of vertical position along the detector is shown in Fig. 11. At two points this parameter falls to the range of 6000 - 7000. However, over most of the crystal it is in the range 8000 - 12000.

When the crystal is used in a spectrometer to measure impurity Doppler linewidths, the rays would be effectively reversed relative to the present measurements, i. e. X-ray at a single wavelength coming from different vertical positions in the plasma and passing through the vertical line of Fig. 9 would converge and be measured at a single point on the detector, located at the source point of our measurements. Thus, the relevant parameter is the average linewidth in our experiment. If we calculate the average resolving power by weighting the data in Fig. 11 according to the X-ray intensity at each point, we obtain an effective resolving power of about 7700. By comparison, the inverse relative Doppler linewidth of argon ions at an impurity temperature of 1.0 keV is, $\lambda/\Delta\lambda_{Doppler} = 2600$. Thus the resolving power of the crystal is fully adequate to measure the typical impurity temperature of argon ions in NSTX plasmas.

Moreover, in practice, a circularly symmetric, spherical crystal such as the one measured here would be masked so that the sensitive area would be a rectangle, e.g. 40 mm x 70 mm, on a 100 mm diameter crystal. Of course, the crystal would be rotated relative to the mask to find the rectangular area of the crystal with the highest resolution before the

crystal was installed in the spectrometer. We can therefore assume that the resolving power of a spectrometer using this crystal would be approximately 10,000.

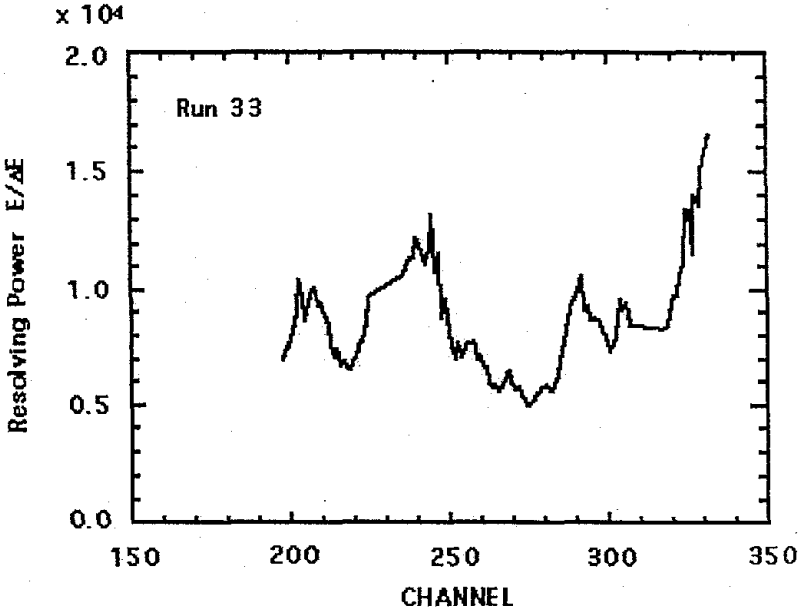

Figure 11 -- Resolving Power vs. Vertical Channel Number

7. Instrument Design

The final task of the phase I program was the preliminary design of the spectrometer to be built in phase II. The spectrometer will consist of the spherical crystal, a two-dimensional position-sensitive detector, reflector and detector positioning mechanisms, and the spectrometer vessel. The spectrometer design is based on the argon line spectrometer designed, in part, by one of the participants in this proposal, M. Bitter, for the German fusion reactor, TEXTOR.

There are two major differences between the TEXTOR spectrometer and the instrument proposed here. The first is that the TEXTOR spectrometer used a cylindrical crystal without sagittal focusing, whereas our proposed spectrometer will use a spherically bent crystal, which focuses the sagittal X-rays resulting in a 1D image of chords through the plasma in the plane perpendicular to the plane of dispersion, the Rowland circle. The second major difference is that the plane of dispersion of the TEXTOR instrument is parallel to the mid-plane of the torus, whereas the Rowland circle of our proposed spectrometer is perpendicular to the mid-plane. Accordingly, our proposed spectrometer will image chords in the horizontal mid-plane of NSTX. If an instrument at NSTX similar to the TEXTOR spectrometer were equipped with a spherical crystal it would image lines of sight in a plane perpendicular to the mid-plane. The physics obtained with these two instruments would be different, but complementary.

Further differences between the two instruments are in the configuration of the interface with the NSTX port, and the size of the Rowland circle. The latter will also change the

length of the tubes that connect the different parts of the instrument. With these exceptions, the TEXTOR and NSTX instruments will be quite similar.

The crystal will be a quartz crystal. Its size will be 125 mm in diameter x 0.75 mm in thickness. The precise value of the radius of curvature of the crystal will be determined once the dimensions of the spectrometer have been determined. It will be approximately 3 meters. The spectrometer will be tuned to the resonance line complex of helium like argon at 4 Å. The interatomic spacing of the reflecting planes of the selected crystal defines the Bragg angle. As such, a quartz crystal reflecting in first order from the (1,1,-2,0) plane with a 2d spacing of 4.9130 Å would have a Bragg angle, coinciding with the center of the argon X-ray wavelength range, of 53.939 degrees.

The X-ray flux from the torus travels down an evacuated tube and enters the spectrometer chamber containing the crystal. It is reflected down another tube to the detector. The center of the crystal and the detector are both located on the Rowland circle. The spectrometer is evacuated in order to prevent absorption of the 3 keV argon X-rays.

The instrument will be isolated from the plasma by a gate valve and a beryllium window. In order to avoid damage to the window, there will be a short tube around the window with a valve so that the pressure on both sides of the window can be equalized when the gate valve is closed. An evacuated stainless steel tube will conduct the X-rays from the entrance aperture to the crystal chamber.

The crystal chamber is a small chamber within which the crystal assembly is mounted. It will have two apertures leading to the NSTX diagnostic port and to the detector chamber, respectively. The plane of the Rowland circle will be vertical. The crystal assembly will be mounted on a set of precision alignment stages. The alignment system will ensure that the crystal assembly, which defines the Rowland circle, is aligned with the NSTX port and the detector. The crystal will be able to translate along the radius of the Rowland circle, and perpendicular to its plane. The crystal assembly will also be able to rotate around the plane of the Rowland circle, about orthogonal axes in order to adjust the Bragg angle. The position and orientation of the crystal assembly will be fed back to the position control system and to the experiment data stream.

The dispersed X-rays will be conducted to the detector via another evacuated tube. The detector will be housed in the detector chamber. The detector will also be mounted to a set of precision alignment stages. The detector will be capable of translating along both axes perpendicular to the line between the crystal and the detector and toward and away from the crystal, so that the center of the detector can be positioned relative to the Rowland circle for best resolution.

As of this writing, there are two possible choices for the X-ray detector. The detector that was used to generate the spectra shown in Figure 5 was designed for high speed plasma imaging. It uses both a specialized image tube and a specialized CCD that represent the current state of the art. In the present application, resolution is more important than speed. Spatial resolution of 0.2 mm or better along the Rowland circle is desirable for line profile measurements. At this time, we envision the use of a two-dimensional position-sensitive proportional counter similar to the detector used in the X-ray tests of the bent crystal described in section 5.2.4. This detector was developed at Brookhaven National Laboratory.

The length of the detector in the direction of dispersion of the spectrum would be between 6 and 8 cm, in order to accommodate the lines **w** and **z**, which are 4.7 cm apart without having to contend with edge effects. The height of the detector in the direction which provides information on the spatial distribution of the plasma parameters should be between 20 and 30 cm. A resolution of 0.2 mm in the dispersion direction is required in order to achieve the spectral resolution needed for the line profiles. This resolution was demonstrated during the X-ray test program. Resolution of the order of millimeters is adequate in the perpendicular, spatial imaging, direction. However, it may be difficult to optimize the dynamic range of the system: the maximum count rate with this instrument would be around 200,000 hertz. A better solution might be to use a stack of smaller multiwire proportional counters of about 6 cm x 1 cm. Such small counters could be optimized with regard to both count rate capability and position sensitivity: count rates on the order of a Megahertz, with a position resolution of 0.2 mm, could be achieved with this configuration, but the electronics would be more extensive. In order to arrive at a budget, we have assumed the use of a single position sensitive proportional counter. However, as the capabilities of X-ray imaging detectors are advancing quite rapidly, we intend to continue investigating the question of an appropriate detector during the early portion of Phase II.

8. Conclusions

We believe that the phase I program was a success.

We demonstrated that a quartz crystal could be bent to a spherical shape around a convex form, thereby eliminating the problems of deviations in the flatness of the crystal, non-uniformities in crystal thickness, and variations in the thickness of the epoxy bonding the crystal to its support form. Optical testing showed that the front surface of the crystal was spherical with an RMS deviation of 1/20 of a wave. X-ray testing showed that the resolving power of this crystal was on the order of 10^4 . We developed a design concept for a spherical crystal spectrometer for use at NSTX and established that it could be built at a cost within the parameters of phase II.

We believe that this program should be continued through phase II.